# Chapter 4

# Numerical cosmic ray transport equation

## 4.1 Introduction

In this chapter an overview of the numerical method used to solve the 2D time-dependent *Parker* (1965) transport equation (TPE) in a spherical coordinate system is given. Also a brief history on numerical models, which compute cosmic ray intensities in the heliosphere, is given. All these models solve the TPE which is a parabolic differential equation. In this work, an unconditionally stable numerical procedure called the ADI method, which is a modification of the Crank-Nicolson method for two spatial dimensions, is used to solve the TPE. This 2D time-dependent model is originally an extension of steady-state 2D model used by *Potgieter* (1984) and *Potgieter and Moraal* (1985) and was extended to a time-dependent 2D model by *Le Roux* (1990) and *Potgieter and Le Roux* (1992). This model is also discussed in this chapter.

## 4.2 A brief history on numerical modulation models

In this section, a brief history of steady-state and time-dependent numerical modulation models are given. Note that this overview is not discussing shock acceleration modulation models since this study deals with galactic particles where TS acceleration is considered not significant. For a detailed history see *Langner* (2004).

The history of modulation models, which solve the TPE numerically, began with *Fisk* (1971) where a one-dimensional (1D) spherically symmetric steady-state model with radial distance as the only spatial variable was developed. Later *Fisk* (1975, 1976) included polar angle dependence and modified his 1D steady-state model to develop a 2D steady-state model, but without drifts. At the same period *Moraal and Gleeson* (1975) and *Cecchini and Quenby* (1975) also developed 2D steady-state models. *Moraal et al.* (1979) and *Jokipii and Kopriva* (1979) improved the 2D steady-state model by including gradient and curvature drifts for a flat HCS. Later *Jokipii and Thomas* (1981), *Potgieter* (1984), *Potgieter and Moraal* (1985), *Burger* (1987) improved the 2D

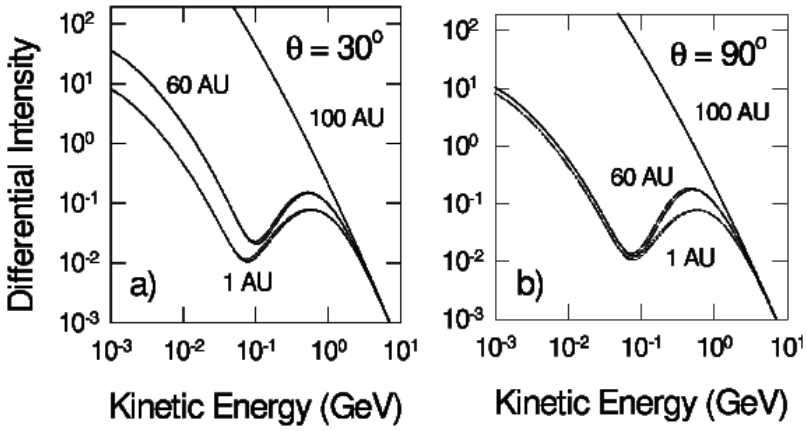


Figure 4.1: Shown are electron spectra computed by 2D and 3D drift models. Left panel shows the differential intensities in units of particles.m$^{-2}$.sr$^{-1}$.s$^{-1}$.MeV$^{-1}$ at 1 AU and 60 AU for a polar angle of $\theta = 30^o$, a tilt angle of $\alpha = 20^o$ and an $A > 0$ polarity cycle. Right panel shows the results for a polar angle of $\theta = 90^o$ (equatorial plane). Note that the spectra for the two models coincide with the LIS specified at 100 AU. From *Ferreira et al.* (1999).

models to emulate the waviness of HCS. This was followed by *Hattingh and Burger* (1995b), *Burger and Hattingh* (1995) who further improved the waviness of HCS by introducing the Wavy Current Sheet (WCS) model. In WCS-model, the 3D drift velocity is replaced by a 2D drift velocity by averaging drift velocity over one solar rotation. A general HCS-approach was later derived by *Langner* (2004) and compared with the WCS-model and found that the difference between the two models decreases with increasing radial distance and with decreasing tilt angles. *Langner* (2004) concluded from his study that the WCS-model is a good approximation and can be used for qualitative studies.

The first 3D steady-state modulation model was developed by *Kota and Jokipii* (1983) including drifts and a fully wavy HCS. Later *Hattingh and Burger* (1995b), *Burger and Hattingh* (1995), *Hattingh* (1998) also developed a 3D steady-state drift model with an improved wavy HCS. These authors compared it with the 3D model developed by *Kota and Jokipii* (1983) and found an excellent compatibility, i.e. within 4% between the two results (*Burger and Hattingh*, 1995). *Hattingh* (1998) and *Ferreira et al.* (1999) did comparative study between the 2D steady-state drift model which included the WCS-model to simulate the HCS and the 3D steady-state model which included an actual wavy current sheet and found a good agreement between the two models.

Figure 4.1 shows the study done by *Ferreira et al.* (1999) showing a comparison between the modulated spectra computed with 2D and 3D drift models with a local interstellar spectra (LIS), in this work specified as heliopause spectra (HPS), assumed at 100 AU. The left panel shows the differential intensities at 1 AU and 60 AU respectively for a polar angle of $\theta = 30^o$ and a tilt angle of $\alpha = 20^o$. The right panel is similar but for a polar angle, $\theta = 90^o$ (equatorial plane). Both solutions in the left and right panel figures are computed during an $A > 0$ polarity cycle because during this cycle, electrons drift in along the HCS and the largest difference

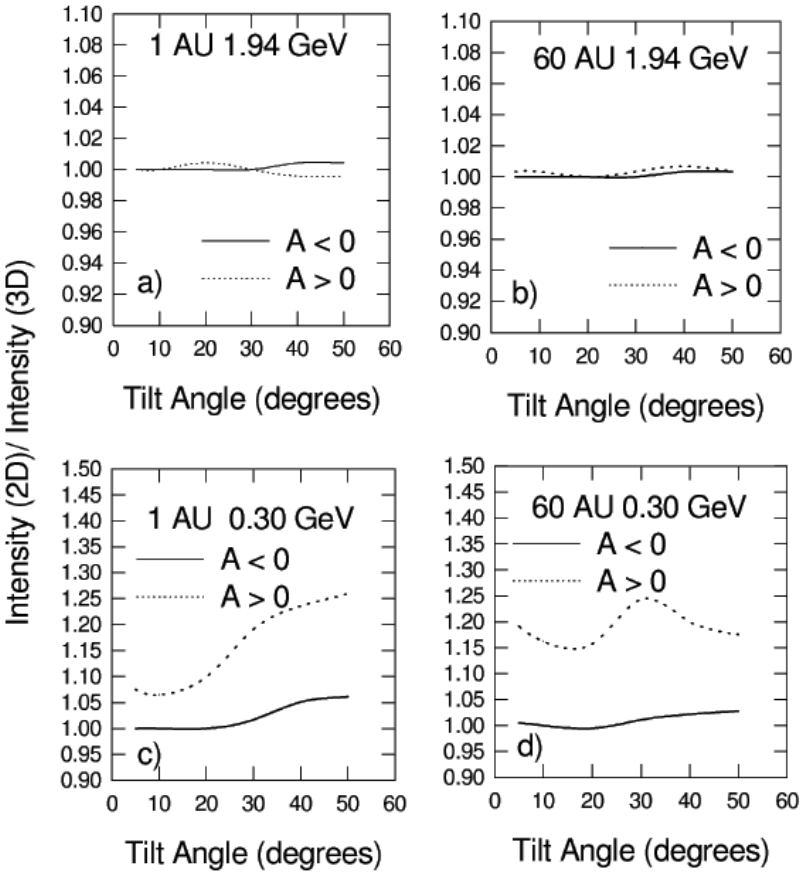


Figure 4.2: The ratio of electron differential intensities computed with 2D and 3D drift models as a function of tilt angle. Top left panel shows the ratio for 1.94 GeV electrons for both the $A > 0$ and $A < 0$ polarity cycles at 1 AU. Top right panel shows the same as top left panel but at 60 AU. Bottom left panel shows the same as top scenarios but for 0.3 GeV electrons at 1 AU and bottom right panel for 0.3 GeV electrons at 60 AU. From *Ferreira et al.* (1999).

between the two models are computed. The left and right panel figures show that the electron spectra computed by both 2D and 3D models coincide despite the use of a complex rigidity dependence for $K_{||}$ and $K_{\perp}$ (*Ferreira et al.*, 1999).

The 2D and 3D model differ significantly in the way that the HCS is treated, so a comparison between the two in terms of tilt angle was done by *Ferreira et al.* (1999). Figure 4.2, from these authors, shows the ratio of computed 2D and 3D differential intensities as a function of tilt angle during both the $A > 0$ and $A < 0$ polarity cycles using same modulation parameters used in computing the results for Figure 4.1. The top left panel of Figure 4.2 shows the ratio for 1.94 GeV electrons for both $A > 0$ and $A < 0$ polarity cycles at 1 AU. The top right panel shows the same but at 60 AU. Both top left and right panel figures, i.e. at 1 AU and 60 AU, shows that for 1.94 GeV electrons the ratio varies with tilt angle to $<\sim 1\%$ for both $A > 0$ and $A < 0$ polarity cycles. However, for 0.3 GeV electrons (bottom left panel of Figure 4.2) during $A < 0$ polarity cycle at 1 AU the ratio varies not more than $\sim 5\%$. But for $A > 0$ polarity cycle the ratio varies to nearly 25%. Bottom right panel shows 0.3 GeV electrons at 60 AU, here during

an $A < 0$ polarity cycle $\sim 3\%$ variation in ratio is calculated but during an $A > 0$ polarity cycle a peculiar tilt dependency is computed for the varying ratio which vary between 15% to 25% comparatively larger than computed at 1 AU. The study by *Ferreira et al.* (1999) showed that during $A < 0$ polarity cycle the solutions were essentially identical but during $A > 0$ polarity cycle the solutions differ to a largest extent of 25% for 0.3 GeV electrons (intermediate energies) but essentially identical for 1.94 GeV (high energies). Also similar studies were done by *Hattingh* (1998). These studies revealed that between the solutions of the 2D and 3D models there are insignificant quantitative difference and no qualitative difference. Thus taking into account the amount of computing time and resources needed for the 3D drift model, the use of the 2D drift model for modulation studies is justified especially when intensities are computed over various solar cycles, as in this work.

Concerning other 3D models, *Fichtner et al.* (2000) and *Ferreira* (2002) developed a 3D steady-state model including a Jovian magnetosphere as a source of low energy electrons. Later *Moeketsi* (2004); *Moeketsi et al.* (2005) included a realistic solar wind speed and coupled it with the perpendicular diffusion coefficient in the polar direction in a 3D steady-state Jovian modulation model. See also the work done by *Nkosi et al.* (2011); *Ndanganeni* (2012).

Shifting to time-dependent models, *Perko and Fisk* (1983) developed the first time-dependent 1D spherically symmetric model. Later *Le Roux* (1990) and *Potgieter and Le Roux* (1992) also developed a time-dependent modulation model including two spatial dimensions for a spherically symmetric time-dependent heliosphere with drifts. The model computed long-term cosmic ray modulation also including the effects of Global Merged Interaction Regions (GMIRs) (see *Potgieter and Le Roux*, 1994; *Le Roux and Potgieter*, 1995). *Kota and Jokipii* (2001b) developed a 3D time-dependent modulation model including drift, diffusion, adiabatic cooling and acceleration. During the same period *Fichtner et al.* (2001) also developed a 3D time-dependent model for electrons neglecting adiabatic cooling of electrons at low energies by doing a momentum averaging of TPE. Afterwards, *Kissmann et al.* (2004) developed a 3D time-dependent model with an approximated energy dependence of the distribution function which therefore allows a study of the effect of Corotating Interaction Regions (CIRs) on energetic electron fluxes. Later, *Sternal et al.* (2011) introduced a Fisk-type HMF into this time-dependent model.

At the same period, hybrid models which used TPE coupled with hydrodynamic (HD) or magnetohydrodynamics (MHD) models were developed by authors like *Scherer and Ferreira* (2005a) and *Florinski and Pogorelov* (2008) including all physical processes in the TPE. *Scherer and Ferreira* (2005a) coupled the 2D time-dependent TPE to a HD model and solved the modulation of anomalous and galactic cosmic ray intensities in the heliosphere over a solar cycle. While *Florinski and Pogorelov* (2008) coupled the 3D time-dependent TPE to a MHD model also simulating cosmic ray transport in the heliosphere but for certain conditions only. Also several self-consistent, time-dependent HD and MHD models of various complexity were also developed by various authors (*Pauls and Zank*, 1996, 1997; *Le Roux and Fichtner*, 1997, 1999b; *Florinski and Jokipii*, 1999; *Florinski et al.*, 2003; *Scherer and Fahr*, 2003a,b; *Pogorelov et al.*, 2008a; *Muller*

*et al.*, 2008, 2009; *Katushkina and Izmodenov*, 2010) also simulating to some extend cosmic ray transport.

For an overview on shock acceleration models with the inclusion of the heliospheric TS, continuous and discontinuous transition of the solar wind, particle acceleration at CIRs, particle acceleration due to diffusive shock acceleration (Fermi I), stochastic acceleration (Fermi II) etc., see e.g. *Jokipii* (1986); *Potgieter and Moraal* (1988); *Kota and Jokipii* (1991); *Steenkamp and Moraal* (1995); *Steenberg and Moraal* (1996); *Langner* (2004); *Strauss* (2010); *Ngobeni and Potgieter* (2010). For more recent models which employs stochastic differential equations (SDEs) to solve the cosmic ray transport see e.g. *Krulls and Achterberg* (1994); *Zhang* (1999); *Florinski and Pogorelov* (2009); *Pei et al.* (2010); *Strauss et al.* (2011, 2012a).

## 4.3 Numerical solution of 2D time-dependent transport equation

### 4.3.1 Numerical scheme

The TPE is a second order linear parabolic partial differential equation and can be solved by the Alternating Direction Implicit (ADI) method developed by *Peaceman and Rachford* (1955) and *Douglas* (1955). The ADI method is a stable numerical procedure with a discretization error of the second order in both space and time (or rigidity) variables. The ADI method is a modification of the Crank-Nicholson finite difference method for two spatial dimensions which computes derivatives at half-way time and/or rigidity intervals on the spatial grid. Later the ADI method was improved by *Douglas* (1962) to solve parabolic equations with three spatial coordinates and a time coordinate.

For the numerical solution the TPE in Equation 3.3 can be written as,

$$\begin{aligned} a_0(r,\theta,P,t)\frac{\partial^2 f}{\partial r^2} + b_0(r,\theta,P,t)\frac{\partial^2 f}{\partial \theta^2} + c_0(r,\theta,P,t)\frac{\partial f}{\partial r} & \\ +d_0(r,\theta,P,t)\frac{\partial f}{\partial \theta} + e_0(r,\theta,P,t)\frac{\partial f}{\partial \ln P} + h_0(r,\theta,P,t)\frac{\partial f}{\partial t} &= 0 \end{aligned} \tag{4.1}$$

where

$$\begin{aligned} a_0(r,\theta,P,t) &= K_{rr}, \\ b_0(r,\theta,P,t) &= \frac{K_{\theta\theta}}{r^2}, \\ c_0(r,\theta,P,t) &= \frac{1}{r^2}\frac{\partial}{\partial r}(r^2 K_{rr}) + \frac{1}{r\sin\theta}\frac{\partial}{\partial \theta}(K_{\theta r}\sin\theta) - V, \\ d_0(r,\theta,P,t) &= \frac{1}{r^2}\frac{\partial}{\partial r}(r K_{r\theta}) + \frac{1}{r^2\sin\theta}\frac{\partial}{\partial \theta}(K_{\theta\theta}\sin\theta), \\ e_0(r,\theta,P,t) &= \frac{1}{3r^2}\frac{\partial}{\partial r}(r^2 V), \\ h_0(r,\theta,P,t) &= -1. \end{aligned}$$

In the case of the steady-state TPE i.e. $\frac{\partial f}{\partial t} = 0$, the rigidity variable is equivalent to the time variable (see *Potgieter*, 1984). The steady-state TPE model of *Potgieter* (1984) and *Potgieter and*

*Moraal* (1985) utilised the standard ADI method and solved two successive finite difference equations. For this study however, a 2D time-dependent model, which utilises a modified ADI method as developed by *Le Roux* (1990) and *Potgieter and Le Roux* (1992), is used to solve TPE with two spatial dimensions, rigidity and time. The advantage of this 2D time-dependent TPE model is that it still has the same number (i.e. two) of successive finite difference equations when compared to the steady-state model, which had to be solved over the whole spatial grid. An alternate way to solve the same problem numerically is to implement the standard ADI method for three spatial coordinates developed by *Douglas* (1962). Where rigidity $P$ is considered as a third spatial coordinate and time $t$ is considered as the only implicit coordinate. As a result of this approach, three finite difference equations are formed which have to be solved in succession. Also two boundary conditions have to be defined for $P$ instead of one as in a modified ADI method. This aspects would make the numerical scheme even more complicated when compared to the modified ADI method.

The two finite difference equations produced by the modified ADI method can be represented as a tridiagonal matrix and then solved by Gauss elimination, utilising a straight forward algorithm. The first finite difference equation (i.e. Equation 4.6) treats only the spatial derivatives in the $r$ directions as implicit in both $P$ and $t$. The first estimated result of $f$ is obtained from this first finite difference equation for a half (intermediate) $P$ and $t$ interval ahead. These estimated results are then substituted into a second finite difference equation (i.e. Equation 4.7) where the spatial derivatives in the $\theta$ directions are treated implicitly in both $P$ and $t$. The results obtained from this equation then gives the predicted values for $f$ at full $P$ and $t$ interval ahead.

To solve the 2D time-dependent TPE (Equation 3.3), a radial grid with $r = i\Delta r$ (where $i = 1, 2, 3, ..., N$) is considered. The distance $r = \Delta r = r_1$ represents near the Sun (inner boundary) while $r = N\Delta r = r_b$ represents the heliospheric modulation boundary (outer boundary). Also a $\theta$ grid with $\theta = j\Delta\theta$ (where $j = 1, 2, 3, ..., M$) running from the solar North Pole $\theta = 0^o$ to the equatorial plane at $\theta = 90^o$ is considered. The rigidity steps decrease logarithmically from an initial large value where modulation is negligible i.e. $\Delta \ln P = 0.08$, while the time steps may start at any chosen time. The distribution function $f$ in terms of the grid points is represented as,

$$\begin{aligned} f(r, \theta, P, t) &= f(i\Delta r, j\Delta\theta, k\Delta P, l\Delta t) \\ &= f_{ijkl} \end{aligned}$$

Note that $f[(i+1)\Delta r, (j-1)\Delta\theta, k\Delta P, l\Delta t]$ is equivalent to $f_{(i+1)(j-1)kl}$ and $f[(i-1)\Delta r, (j+1)\Delta\theta, (k+1)\Delta P, (l+1)\Delta t]$ is equivalent to $f_{(i-1)(j+1)k'l'}$ etc. Also note that $k'$ and $l'$ is used instead of $(k+1)$ and $(l+1)$ since $k$ and $l$ both have only $+1$ interval when compared to $i$ and $j$ which has both $\pm 1$ intervals. Further on in the text, to save space and for greater clarity, these notations are used.

The Taylor expansion of a function $f(x)$, up to first three terms about an interval $\Delta x$, are given

by,

$$f(x-\Delta x) = f(x) - f'(x)\Delta x + \frac{f''(x)(\Delta x)^2}{2} \tag{4.2}$$

$$f(x+\Delta x) = f(x) + f'(x)\Delta x + \frac{f''(x)(\Delta x)^2}{2} \tag{4.3}$$

The first order $f'(x)$ and the second order $f''(x)$ derivatives centred around $x$ can be obtained by subtracting and adding Equations 4.2 and 4.3.

$$f'(x) = \frac{f(x+\Delta x) - f(x-\Delta x)}{2\Delta x} \tag{4.4}$$

$$f''(x) = \frac{f(x+\Delta x) - 2f(x) + f(x-\Delta x)}{(\Delta x)^2}. \tag{4.5}$$

The first and second finite difference equations of TPE are obtained by substituting the above first and second order derivative equivalent for $r$, $\theta$, $P$ and $t$ in Equation 4.1. For the first finite difference equation, the derivatives in the $r$ direction specified at both half a $P$ interval and $t$ interval ahead are obtained by substituting a quarter of the central finite difference (Equations 4.4 and 4.5) analogue of $r$ in Equation 4.1. The derivatives in the $\theta$ direction are also specified at half a $t$ interval ahead, but at the present $P$ value and therefore only half of the central finite differences in $\theta$ are substituted in Equation 4.1. As a result Equation 4.1 becomes,

$$\begin{aligned}
&\frac{a_0}{4(\Delta r)^2}\Big[(f_{(i+1)jkl} - 2f_{ijkl} + f_{(i-1)jkl}) + (f^*_{(i+1)jk'l} - 2f^*_{ijk'l} + f^*_{(i-1)jk'l}) \\
&\qquad + (f_{(i+1)jkl'} - 2f_{ijkl'} + f_{(i-1)jkl'}) + (f^*_{(i+1)jk'l'} - 2f^*_{ijk'l'} + f^*_{(i-1)jk'l'})\Big] \\
&+\frac{b_0}{2(\Delta\theta)^2}\Big[(f_{i(j+1)kl} - 2f_{ijkl} + f_{i(j-1)kl}) + (f_{i(j+1)kl'} - 2f_{ijkl'} + f_{i(j-1)kl'})\Big] \\
&+\frac{c_0}{8\Delta r}\Big[(f_{(i+1)jkl} - f_{(i-1)jkl}) + (f^*_{(i+1)jk'l} - f^*_{(i-1)jk'l}) \\
&\qquad + (f_{(i+1)jkl'} - f_{(i-1)jkl'}) + (f^*_{(i+1)jk'l'} - f^*_{(i-1)jk'l'})\Big] \\
&+\frac{d_0}{4\Delta\theta}\Big[(f_{i(j+1)kl} - f_{i(j-1)kl}) + (f_{i(j+1)kl'} - f_{i(j-1)kl'})\Big] \\
&+\frac{e_0}{2(-\Delta \ln P)}\Big[(f^*_{ijk'l} - f_{ijkl}) + (f^*_{ijk'l'} - f_{ijkl'})\Big] \\
&+\frac{h_0}{2(\Delta t)}\Big[(f_{ijkl'} - f_{ijkl}) + (f^*_{ijk'l'} - f^*_{ijk'l})\Big] = 0 \\
&\text{where} \quad i = 1, 2, 3, ...., (N-1) \quad \text{and} \quad j = 1, 2, 3, ...., M.
\end{aligned} \tag{4.6}$$

Here $f_{ijkl}$ is the presently known solution for the $k$th $P$-step at $l$th $t$-step and $f_{ijkl'}$ is the predicted solution for the $k$th $P$-step at $(l+1)$th $t$-step. Also $f^*_{ijk'l}$ and $f^*_{ijk'l'}$ are the presently known intermediate (estimate) solution for the $(k+1)$th $P$-step at $l$th $t$-step and the intermediate predicted solution for the $(k+1)$th $P$-step at $(l+1)$th $t$-step respectively.

The spatial derivatives in Equation 4.6 are treated implicitly in both $P$ and $t$ in the radial direction while the spatial derivatives in the $\theta$ direction are treated implicitly only in $t$ (not in $P$).

For each time step $t$, from $l = 1, 2, 3, ....\infty$, at the rigidity from $k = 1, 2, 3, ...., N_P$ Equation 4.6 is solved for the spatial grid $(i\Delta r, j\Delta\theta)$.

The second finite difference equation is then obtained by assigning the derivatives in the $\theta$ direction at both full $P$ interval and $t$ interval ahead by substituting a quarter of the central finite difference analogue of $\theta$ in Equation 4.1. This time the derivatives in $\theta$ direction is treated implicitly in both $t$ and $P$. The resulting second finite difference equation is given as,

$$
\begin{aligned}
&\frac{a_0}{4(\Delta r)^2}\Big[(f_{(i+1)jkl} - 2f_{ijkl} + f_{(i-1)jkl}) + (f^{*}_{(i+1)jk'l} - 2f^{*}_{ijk'l} + f^{*}_{(i-1)jk'l}) \\
&\qquad + (f_{(i+1)jkl'} - 2f_{ijkl'} + f_{(i-1)jkl'}) + (f^{*}_{(i+1)jk'l'} - 2f^{*}_{ijk'l'} + f^{*}_{(i-1)jk'l'})\Big] \\
&+\frac{b_0}{4(\Delta\theta)^2}\Big[(f_{i(j+1)kl} - 2f_{ijkl} + f_{i(j-1)kl}) + (f_{i(j+1)kl'} - 2f_{ijkl'} + f_{i(j-1)kl'}) \\
&\qquad + (f^{**}_{i(j+1)k'l} - 2f^{**}_{ijk'l} + f^{**}_{i(j-1)k'l}) + (f^{**}_{i(j+1)k'l'} - 2f^{**}_{ijk'l'} + f^{**}_{i(j-1)k'l'})\Big] \\
&+\frac{c_0}{8\Delta r}\Big[(f_{(i+1)jkl} - f_{(i-1)jkl}) + (f^{*}_{(i+1)jk'l} - f^{*}_{(i-1)jk'l}) \\
&\qquad + (f_{(i+1)jkl'} - f_{(i-1)jkl'}) + (f^{*}_{(i+1)jk'l'} - f^{*}_{(i-1)jk'l'})\Big] \\
&+\frac{d_0}{8\Delta\theta}\Big[(f_{i(j+1)kl} - f_{i(j-1)kl}) + (f_{i(j+1)kl'} - f_{i(j-1)kl'}) \\
&\qquad + (f^{**}_{i(j+1)k'l} - f^{**}_{i(j-1)k'l}) + (f^{**}_{i(j+1)k'l'} - f^{**}_{i(j-1)k'l'})\Big] \\
&+\frac{e_0}{2(-\Delta\ln P)}\Big[(f^{**}_{ijk'l} - f_{ijkl}) + (f^{**}_{ijk'l'} - f_{ijkl'})\Big] \\
&+\frac{h_0}{2(\Delta t)}\Big[(f_{ijkl'} - f_{ijkl}) + (f^{**}_{ijk'l'} - f^{**}_{ijk'l})\Big] = 0 \\
&\text{where} \quad i = 1, 2, 3, ...., (N-1) \quad \text{and} \quad j = 1, 2, 3, ...., M.
\end{aligned}
\tag{4.7}
$$

Here $f^{**}_{ijk'l}$ and $f^{**}_{ijk'l'}$ are the presently known solution for the $(k+1)$th $P$-step at $l$th $t$-step and the predicted solution for the $(k+1)$th $P$-step at $(l+1)$th $t$-step, respectively. The grid point $(i, j, k+\frac{1}{2}, l+\frac{1}{2})$ where the spatial derivatives specified in $r$-direction and $\theta$-direction are treated implicit in both $P$ and $t$, is used to calculate the coefficients in both Equation 4.6 and Equation 4.7. For each time step $t$, from $l = 1, 2, 3, ....\infty$, at the rigidity from $k = 1, 2, 3, ...., N_P$, the second difference Equation 4.7 is also solved over the whole spatial grid $(i\Delta r, j\Delta\theta)$.

The first and second finite difference equations thus form a system of tridagonal linear equations which can be easily solved by Gauss elimination method. Using Gauss elimination method the estimated values, $f^{*}_{ijk'l'}$ in Equation 4.6, is calculated. Then this results (i.e. $f^{*}_{ijk'l'}$) are incorporated into Equation 4.7 to find the predicted values of $f^{**}_{ijk'l'}$. However, in order to solve these system of tridiagonal linear equations using a Gauss elimination method, initial and boundary conditions have to be defined.

### 4.3.2 Boundary conditions and initial values

A spherical heliosphere with a steady-state condition is assumed at time $t = 0$, preferably a solar minimum period. This assumption makes the heliosphere relatively stable and undisturbed at initial state when compared to a solar maximum period where a polarity reversal of HMF takes place. This steady-state condition is computed by the standard ADI method as used by *Potgieter* (1984). Also the model assumes that at high rigidity values there is no cosmic ray modulation i.e. $f = f_g$, the HPS, over the entire spatial grid at $k = 1$. The HPS values are assumed to be time independent so that the initial condition in $P$ is used at each time step in the modified ADI method.

The boundary conditions used are as follows,

- The inner modulation boundary, $r_1$ $(r_1 = i\Delta r, \text{ when } i = 1)$ was chosen to be located at a distance near the surface of the Sun i.e. $r_1 > r_\odot$. Also a reflective boundary was assumed which imply that no particles enter or leave the Sun.

$$\left[\frac{\partial f}{\partial r}\right]_{r=r_1} = 0. \tag{4.8}$$

  *Siluszyk and Alania* (2001) showed that an absorbing Sun could be a more appropriate boundary condition. i.e.

$$\left[\frac{\partial f}{\partial r}\right]_{r=r_1} \neq 0.$$

  The comparison between the model with reflective and absorbing Sun showed that the results are only sensitive for the first 0.25 AU to this boundary conditions (see e.g. *Potgieter*, 1984; *Le Roux*, 1990; *Siluszyk and Alania*, 2001; *Ferreira*, 2002).

- For the outer heliospheric boundary, $r_b$ $(r_b = i\Delta r, \text{ when } i = N)$, a HPS for a particular species of cosmic rays is used as the input spectrum (see Chapter 6 for a discussion on HPS).

$$f(r_b, \theta, P, t) = f_g. \tag{4.9}$$

- The polar angle boundary condition at $0^o$ and $90^o$, ($\theta = j\Delta\theta = 0^o, \text{ when } j = 1$ and $\theta = 90^o, \text{ when } j = M$). The heliosphere is assumed to be symmetrical about the poles and the equitorial plane, so the boundary conditions at the polar region and the equatorial plane is specified as,

$$\left[\frac{\partial f}{\partial \theta}\right]_{\theta=0^o,90^o} = 0. \tag{4.10}$$

### 4.3.3 Numerical transport equation

The first finite equation (Equation 4.6) of TPE can be rearranged as given below,

$$\begin{aligned} A_i f^*_{(i-1)jk'l'} + B_i f^*_{ijk'l'} + C_i f^*_{(i+1)jk'l'} = \quad & -D_{1,i} f_{(i-1)jkl} - D_{2,i} f_{ijkl} - D_{3,i} f_{(i+1)jkl} \\ & -D_{4,i} f^*_{(i-1)jk'l} - D_{5,i} f^*_{ijk'l} - D_{6,i} f^*_{(i+1)jk'l} \\ & -D_{7,i} f_{(i-1)jkl'} - D_{8,i} f_{ijkl'} - D_{9,i} f_{(i+1)jkl'} \\ & -D_{10,i} f_{i(j-1)kl} - D_{11,i} f_{i(j+1)kl} \\ & -D_{12,i} f_{i(j-1)kl'} - D_{13,i} f_{i(j+1)kl'} \end{aligned} \tag{4.11}$$

Where $i = 1, 2, 3, ...., (N-1)$ and $j = 1, 2, 3, ...., M$.

Here,

$$\begin{aligned} A_i &= \frac{a_0}{4(\Delta r)^2} - \frac{c_0}{8(\Delta r)}, \\ B_i &= -\frac{a_0}{2(\Delta r)^2} - \frac{e_0}{2(\Delta \ln P)} + \frac{h_0}{2(\Delta t)}, \\ C_i &= \frac{a_0}{4(\Delta r)^2} + \frac{c_0}{8(\Delta r)}, \\ D_{1,i} &= A_i \\ D_{2,i} &= -\frac{a_0}{2(\Delta r)^2} - \frac{b_0}{(\Delta \theta)^2} + \frac{e_0}{2(\Delta \ln P)} - \frac{h_0}{2(\Delta t)}, \\ D_{3,i} &= C_i, \\ D_{4,i} &= A_i, \\ D_{5,i} &= -\frac{a_0}{2(\Delta r)^2} - \frac{e_0}{2(\Delta \ln P)} - \frac{h_0}{2(\Delta t)}, \\ D_{6,i} &= C_i, \\ D_{7,i} &= A_i, \\ D_{8,i} &= -\frac{a_0}{2(\Delta r)^2} - \frac{b_0}{(\Delta \theta)^2} + \frac{e_0}{2(\Delta \ln P)} + \frac{h_0}{2(\Delta t)}, \\ D_{9,i} &= C_i, \\ D_{10,i} &= \frac{b_0}{2(\Delta \theta)^2} - \frac{d_0}{4(\Delta \theta)}, \\ D_{11,i} &= \frac{b_0}{2(\Delta \theta)^2} + \frac{d_0}{4(\Delta \theta)}, \\ D_{12,i} &= D_{10,i}, \\ D_{13,i} &= D_{11,i}. \end{aligned}$$

A second finite difference equation can be obtained by subtracting Equation 4.6 from Equation 4.7,

$$\begin{aligned} A'_j f^{**}_{i(j-1)k'l'} + B'_j f^{**}_{ijk'l'} + C'_j f^{**}_{i(j+1)k'l'} = \quad & -D'_{1,j} f_{i(j-1)kl} - D'_{2,j} f_{ijkl} - D'_{3,j} f_{i(j+1)kl} \\ & -D'_{4,j} f^{**}_{i(j-1)k'l} - D'_{5,j} f^{**}_{ijk'l} - D'_{6,j} f^{**}_{i(j+1)k'l} \\ & -D'_{7,j} f_{i(j-1)kl'} - D'_{8,j} f_{ijkl'} - D'_{9,j} f_{i(j+1)kl'} \\ & -D'_{10,j} f^{*}_{ijk'l} - D'_{11,j} f^{*}_{ijk'l'} \end{aligned} \tag{4.12}$$

Where $j = 1, 2, 3, ...., M$ and $i = 1, 2, 3, ...., (N-1)$.

Here,

$$\begin{aligned} A'_j &= \frac{b_0}{4(\Delta\theta)^2} - \frac{d_0}{8(\Delta\theta)}, \\ B'_j &= -\frac{b_0}{2(\Delta\theta)^2} - \frac{e_0}{2(\Delta \ln P)} + \frac{h_0}{2(\Delta t)}, \\ C'_j &= \frac{b_0}{4(\Delta\theta)^2} + \frac{d_0}{8(\Delta\theta)}, \\ D'_{1,j} &= -A'_j, \\ D'_{2,j} &= \frac{b_0}{2(\Delta\theta)^2}, \\ D'_{3,j} &= -C'_j, \\ D'_{4,j} &= A'_j, \\ D'_{5,j} &= -\frac{b_0}{2(\Delta\theta)^2} - \frac{e_0}{2(\Delta \ln P)} - \frac{h_0}{2(\Delta t)}, \\ D'_{6,j} &= C'_j, \\ D'_{7,j} &= -A'_j, \\ D'_{8,j} &= D'_{2j}, \\ D'_{9,j} &= -C'_j, \\ D'_{10,j} &= \frac{e_0}{2(\Delta \ln P)} + \frac{h_0}{2(\Delta t)}, \\ D'_{11,j} &= \frac{e_0}{2(\Delta \ln P)} - \frac{h_0}{2(\Delta t)}. \end{aligned}$$

After including the boundary conditions, the first finite difference Equation 4.11 forms a system of $(N-1)$ linear equations. These linear equations can be represented as a tridiagonal matrix and then solved with the Gauss elimination method for $j = 1, 2, 3, ...., M$.

$$\begin{bmatrix} B_1 & (A_1+C_1) & 0 & .... & 0 & 0 & 0 \\ A_2 & B_2 & C_2 & .... & 0 & 0 & 0 \\ \vdots & \vdots & \vdots & \ddots & \vdots & \vdots & \vdots \\ 0 & 0 & 0 & .... & A_{(N-2)} & B_{(N-2)} & C_{(N-2)} \\ 0 & 0 & 0 & .... & 0 & A_{(N-1)} & B_{(N-1)} \end{bmatrix} \begin{bmatrix} f^*_{1jk'l'} \\ f^*_{2jk'l'} \\ \vdots \\ f^*_{(N-2)jk'l'} \\ f^*_{(N-1)jk'l'} \end{bmatrix} = \quad (4.13)$$

$$- \begin{bmatrix} D_{2,1} & (D_{1,1}+D_{3,1}) & 0 & .... & 0 & 0 & 0 \\ D_{1,2} & D_{2,2} & D_{3,2} & .... & 0 & 0 & 0 \\ \vdots & \vdots & \vdots & \ddots & \vdots & \vdots & \vdots \\ 0 & 0 & 0 & .... & D_{1,(N-2)} & D_{2,(N-2)} & D_{3,(N-2)} \\ 0 & 0 & 0 & .... & 0 & D_{1,(N-1)} & D_{2,(N-1)} \end{bmatrix} \begin{bmatrix} f_{1jkl} \\ f_{2jkl} \\ \vdots \\ f_{(N-2)jkl} \\ f_{(N-1)jkl} \end{bmatrix}$$

$$- \begin{bmatrix} D_{5,1} & (D_{4,1}+D_{6,1}) & 0 & .... & 0 & 0 & 0 \\ D_{4,2} & D_{5,2} & D_{6,2} & .... & 0 & 0 & 0 \\ \vdots & \vdots & \vdots & \ddots & \vdots & \vdots & \vdots \\ 0 & 0 & 0 & .... & D_{4,(N-2)} & D_{5,(N-2)} & D_{6,(N-2)} \\ 0 & 0 & 0 & .... & 0 & D_{4,(N-1)} & D_{5,(N-1)} \end{bmatrix} \begin{bmatrix} f^*_{1jk'l} \\ f^*_{2jk'l} \\ \vdots \\ f^*_{(N-2)jk'l} \\ f^*_{(N-1)jk'l} \end{bmatrix}$$

$$- \begin{bmatrix} D_{8,1} & (D_{7,1}+D_{9,1}) & 0 & .... & 0 & 0 & 0 \\ D_{7,2} & D_{8,2} & D_{9,2} & .... & 0 & 0 & 0 \\ \vdots & \vdots & \vdots & \ddots & \vdots & \vdots & \vdots \\ 0 & 0 & 0 & .... & D_{7,(N-2)} & D_{8,(N-2)} & D_{9,(N-2)} \\ 0 & 0 & 0 & .... & 0 & D_{7,(N-1)} & D_{8,(N-1)} \end{bmatrix} \begin{bmatrix} f_{1jkl'} \\ f_{2jkl'} \\ \vdots \\ f_{(N-2)jkl'} \\ f_{(N-1)jkl'} \end{bmatrix}$$

$$- \begin{bmatrix} D_{10,1} & (0 & 0 & .... & 0 & 0 & 0 \\ 0 & D_{10,2} & 0 & .... & 0 & 0 & 0 \\ \vdots & \vdots & \vdots & \ddots & \vdots & \vdots & \vdots \\ 0 & 0 & 0 & .... & 0 & D_{10,(N-2)} & 0 \\ 0 & 0 & 0 & .... & 0 & 0 & D_{10,(N-1)} \end{bmatrix} \begin{bmatrix} f_{1(j-1)kl} \\ f_{2(j-1)kl} \\ \vdots \\ f_{(N-2)(j-1)kl} \\ f_{(N-1)(j-1)kl} \end{bmatrix}$$

$$- \begin{bmatrix} D_{11,1} & (0 & 0 & .... & 0 & 0 & 0 \\ 0 & D_{11,2} & 0 & .... & 0 & 0 & 0 \\ \vdots & \vdots & \vdots & \ddots & \vdots & \vdots & \vdots \\ 0 & 0 & 0 & .... & 0 & D_{11,(N-2)} & 0 \\ 0 & 0 & 0 & .... & 0 & 0 & D_{11,(N-1)} \end{bmatrix} \begin{bmatrix} f_{1(j+1)kl} \\ f_{2(j+1)kl} \\ \vdots \\ f_{(N-2)(j+1)kl} \\ f_{(N-1)(j+1)kl} \end{bmatrix}$$

$$
- \begin{bmatrix} D_{12,1} & (0 & 0 & .... & 0 & 0 & 0 \\ 0 & D_{12,2} & 0 & .... & 0 & 0 & 0 \\ \vdots & \vdots & \vdots & \ddots & \vdots & \vdots & \vdots \\ 0 & 0 & 0 & .... & 0 & D_{12,(N-2)} & 0 \\ 0 & 0 & 0 & .... & 0 & 0 & D_{12,(N-1)} \end{bmatrix} \begin{bmatrix} f_{1(j-1)kl'} \\ f_{2(j-1)kl'} \\ \vdots \\ f_{(N-2)(j-1)kl'} \\ f_{(N-1)(j-1)kl'} \end{bmatrix}
$$

$$
- \begin{bmatrix} D_{13,1} & (0 & 0 & .... & 0 & 0 & 0 \\ 0 & D_{13,2} & 0 & .... & 0 & 0 & 0 \\ \vdots & \vdots & \vdots & \ddots & \vdots & \vdots & \vdots \\ 0 & 0 & 0 & .... & 0 & D_{13,(N-2)} & 0 \\ 0 & 0 & 0 & .... & 0 & 0 & D_{13,(N-1)} \end{bmatrix} \begin{bmatrix} f_{1(j+1)kl'} \\ f_{2(j+1)kl'} \\ \vdots \\ f_{(N-2)(j+1)kl'} \\ f_{(N-1)(j+1)kl'} \end{bmatrix}
$$

$$
\begin{aligned}
X_1 &= \frac{A_1 + C_1}{B_1}; \\
X_i &= \frac{C_i}{B_i - A_i X_{i-1}}; \quad i = 2, 3, ..., N-1;
\end{aligned}
$$

and

$$
\begin{aligned}
Y_1 &= \frac{D_1}{B_1}; \\
Y_i &= \frac{D_i - A_i Y_{i-1}}{B_i - A_i X_{i-1}}; \quad i = 2, 3, ..., N-1;
\end{aligned}
$$

with

$$
\begin{aligned}
D_i = & -D_{1,i} f_{(i-1)jkl} - D_{2,i} f_{ijkl} - D_{3,i} f_{(i+1)jkl} \\
& -D_{4,i} f^*_{(i-1)jk'l} - D_{5,i} f^*_{ijk'l} - D_{6,i} f^*_{(i+1)jk'l} \\
& -D_{7,i} f_{(i-1)jkl'} - D_{8,i} f_{ijkl'} - D_{9,i} f_{(i+1)jkl'} \\
& -D_{10,i} f_{i(j-1)kl} - D_{11,i} f_{i(j+1)kl} \\
& -D_{12,i} f_{i(j-1)kl'} - D_{13,i} f_{i(j+1)kl'}
\end{aligned}
$$

The boundary conditions, with the $P$ and $t$ indices suppressed, are,

$$
f_{0j} = f_{2j}; \quad f_{Nj} = f_g; \quad f_{i0} = f_{i2}; \quad f_{i(M-1)} = f_{i(M+1)}
$$

The intermediate (or estimated) solution is then,

$$
f^*_{(N-i)jk'l'} = Y_{(N-i)} - X_{(N-i)} f^*_{(N-i+1)jk'l'} \tag{4.14}
$$

$$
\text{where} \quad i = 1, 2, 3, ...., (N-1) \quad \text{and} \quad j = 1, 2, 3, ...., M.
$$

The solution of the second system of $M$ linear Equations 4.12 is obtained by calculating for

$i = 1, 2, 3, ...., (N-1)$.

$$\begin{bmatrix} B'_1 & (A'_1+C'_1) & 0 & .... & 0 & 0 & 0 \\ A'_2 & B'_2 & C'_2 & .... & 0 & 0 & 0 \\ \vdots & \vdots & \vdots & \ddots & \vdots & \vdots & \vdots \\ 0 & 0 & 0 & .... & A'_{(M-1)} & B'_{(M-1)} & C'_{(M-1)} \\ 0 & 0 & 0 & .... & 0 & A'_M & B'_M \end{bmatrix} \begin{bmatrix} f^{**}_{i1k'l'} \\ f^{**}_{i2k'l'} \\ \vdots \\ f^{**}_{i(M-1)k'l'} \\ f^{**}_{iMk'l'} \end{bmatrix} = \quad (4.15)$$

$$- \begin{bmatrix} D'_{2,1} & (D'_{1,1}+D'_{3,1}) & 0 & .... & 0 & 0 & 0 \\ D'_{1,2} & D'_{2,2} & D'_{3,2} & .... & 0 & 0 & 0 \\ \vdots & \vdots & \vdots & \ddots & \vdots & \vdots & \vdots \\ 0 & 0 & 0 & .... & D'_{1,(M-1)} & D'_{2,(M-1)} & D'_{3,(M-1)} \\ 0 & 0 & 0 & .... & 0 & D'_{1,M} & D'_{2,M} \end{bmatrix} \begin{bmatrix} f_{i1kl} \\ f_{i2kl} \\ \vdots \\ f_{i(M-1)kl} \\ f_{iMkl} \end{bmatrix}$$

$$- \begin{bmatrix} D'_{5,1} & (D'_{4,1}+D'_{6,1}) & 0 & .... & 0 & 0 & 0 \\ D'_{4,2} & D'_{5,2} & D'_{6,2} & .... & 0 & 0 & 0 \\ \vdots & \vdots & \vdots & \ddots & \vdots & \vdots & \vdots \\ 0 & 0 & 0 & .... & D'_{4,(M-1)} & D'_{5,(M-1)} & D'_{6,(M-1)} \\ 0 & 0 & 0 & .... & 0 & D'_{4,M} & D'_{5,M} \end{bmatrix} \begin{bmatrix} f^{**}_{i1k'l} \\ f^{**}_{i2k'l} \\ \vdots \\ f^{**}_{i(M-1)k'l} \\ f^{**}_{iMk'l} \end{bmatrix}$$

$$- \begin{bmatrix} D'_{8,1} & (D'_{7,1}+D'_{9,1}) & 0 & .... & 0 & 0 & 0 \\ D'_{7,2} & D'_{8,2} & D'_{9,2} & .... & 0 & 0 & 0 \\ \vdots & \vdots & \vdots & \ddots & \vdots & \vdots & \vdots \\ 0 & 0 & 0 & .... & D'_{7,(M-1)} & D'_{8,(M-1)} & D'_{9,(M-1)} \\ 0 & 0 & 0 & .... & 0 & D'_{7,M} & D'_{8,M} \end{bmatrix} \begin{bmatrix} f_{i1kl'} \\ f_{i2kl'} \\ \vdots \\ f_{i(M-1)kl'} \\ f_{iMkl'} \end{bmatrix}$$

$$- \begin{bmatrix} D_{10,1} & (0 & 0 & .... & 0 & 0 & 0 \\ 0 & D_{10,2} & 0 & .... & 0 & 0 & 0 \\ \vdots & \vdots & \vdots & \ddots & \vdots & \vdots & \vdots \\ 0 & 0 & 0 & .... & 0 & D_{10,(M-1)} & 0 \\ 0 & 0 & 0 & .... & 0 & 0 & D_{10,M} \end{bmatrix} \begin{bmatrix} f^{*}_{i1k'l} \\ f^{*}_{i2k'l} \\ \vdots \\ f^{*}_{i(M-1)k'l} \\ f^{*}_{iMk'l} \end{bmatrix}$$

$$- \begin{bmatrix} D_{11,1} & (0 & 0 & .... & 0 & 0 & 0 \\ 0 & D_{11,2} & 0 & .... & 0 & 0 & 0 \\ \vdots & \vdots & \vdots & \ddots & \vdots & \vdots & \vdots \\ 0 & 0 & 0 & .... & 0 & D_{11,(M-1)} & 0 \\ 0 & 0 & 0 & .... & 0 & 0 & D_{11,M} \end{bmatrix} \begin{bmatrix} f^{*}_{i1k'l'} \\ f^{*}_{i2k'l'} \\ \vdots \\ f^{*}_{i(M-1)k'l'} \\ f^{*}_{iMk'l'} \end{bmatrix}$$

$$\begin{aligned} X'_1 &= \frac{A'_1+C'_1}{B'_1}; \\ X'_j &= \frac{C'_j}{B'_j - A'_j X'_{j-1}}; \quad j = 1, 2, 3, ...., (M-1); \end{aligned}$$

and

$$\begin{aligned} Y'_1 &= \frac{D'_1}{B'_1}; \\ Y'_j &= \frac{D'_j - A'_j Y'_{j-1}}{B'_j - A'_j X_{j-1}}; \quad j = 1, 2, 3, ...., (M-1); \end{aligned}$$

with

$$\begin{aligned} D'_J &= -D'_{1,j} f_{i(j-1)kl} - D'_{2,j} f_{ijkl} - D'_{3,j} f_{i(j+1)kl} \\ &\quad -D'_{4,j} f^{**}_{i(j-1)k'l} - D'_{5,j} f^{**}_{ijk'l} - D'_{6,j} f^{**}_{i(j+1)k'l} \\ &\quad -D'_{7,j} f_{i(j-1)kl'} - D'_{8,j} f_{ijkl'} - D'_{9,j} f_{i(j+1)kl'} \\ &\quad -D'_{10,j} f^{*}_{ijk'l} - D'_{11,j} f^{*}_{ijk'l'} \end{aligned}$$

Only the following boundary conditions are needed in this case:

$$f_{i0} = f_{i2}; \quad f_{i(M-1)} = f_{i(M+1)}$$

The final solution then is

$$f^{**}_{i(M-j)k'l'} = Y'_{(M-j)} - X'_{(M-j)} f^{**}_{i(M-j+1)k'l'} \tag{4.16}$$

$$\text{where} \quad j = 1, 2, 3, ...., (M-1). \quad \text{and} \quad i = 1, 2, 3, ...., (N-1)$$

with the solution in the neutral sheet, where $j = M$;

$$f^{**}_{iMk'l'} = \frac{D'_M - (A'_M + C'_M) Y'_(M-1)}{B'_M - (A'_M + C'_M) X'_(M-1)}$$

with

$$\begin{aligned} D'_M &= -(D'_{1,M} + D'_{3,M}) f_{i(M-1)kl} - D'_{2,M} f_{iMkl} - (D'_{4,M} + D'_{6,M}) f_{i(M-1)k'l} \\ &\quad -D'_{5,M} f^{*}_{iMk'l} - (D'_{7,M} + D'_{9,M}) f_{i(M-1)kl'} \\ &\quad -D'_{8,M} f_{iMkl'} - D'_{10,M} f^{*}_{iMk'l} - D'_{11,M} f^{*}_{iMk'l'}. \end{aligned}$$

## 4.4 Summary

This chapter gave a brief overview on the history of different cosmic ray modulation models. These models had evolved in the last four decades from a 1D steady-state model to recent 3D time-dependent models. A comparative study between the 2D time-dependent drift model and the 3D steady-state drift model by *Hattingh* (1998) and *Ferreira et al.* (1999) revealed the insignificant differences between the 2D drift model compared to a 3D approach. These authors found that during $A < 0$ polarity cycle the 2D and 3D electron differential intensity solutions were essentially identical and during $A > 0$ polarity cycle the solutions differ to a largest extent of ∼25% for intermediate energies and essentially identical for high energies. However, taking into account the amount of computing time and resources needed for the 3D drift model, the

use of the 2D drift model for long-term modulation studies is justified due to the insignificant quantitative difference and no qualitative difference between the two models.

The numerical scheme used in this work to solve the 2D time-dependent *Parker* (1965) transport equation (TPE) was discussed. A modified ADI numerical scheme developed by *Le Roux* (1990) and *Potgieter and Le Roux* (1992), by including time-dependence to the steady-state model of *Potgieter* (1984) and *Potgieter and Moraal* (1985), is used for this work. This model solves the TPE for two spatial coordinates, a rigidity and a time coordinate. The advantage of this modified ADI method is that it still has the same number of successive finite difference equations when compared to the standard ADI method, which had to be solved over the whole spatial grid.

A spherically symmetric heliosphere is assumed in this numerical model. The radial grid is assumed as $r = i\Delta r$ and the polar grid is assumed as $\theta = j\Delta\theta$ with $i = 1, 2, 3, ...., N$ and $j = 1, 2, 3, ...., M$. The rigidity was chosen from a high value with no modulation is assumed as an initial condition which then decreases as $\Delta \ln P = 0.08$. The boundary conditions are specified with $r_1$, the inner heliospheric boundary assuming a reflective Sun which means that no particles can enter or leave this boundary. Outer boundary, $r_b$ is assumed where the HPS for the particular cosmic ray species is used as the input spectrum, $f_g$. The two finite difference equations produced as a result of the modified ADI approach can be represented as a tridagonal matrix which can be solved using Gauss elimination method in succession such that the results (estimate values) from the first finite difference equation is implemented into the second finite difference equation to find the predicted values of the distribution function at a full $P$ and $t$ step ahead.